EIC BEAM DYNAMICS CHALLENGES*

D. Xu†, E. C. Aschenauer, G. Bassi, J. Beebe-Wang, J. S. Berg, W. Bergan, M. Blaskiewicz,
A. Blednykh, J. M. Brennan, S. Brooks, K. A. Brown, Z. Conway, K. A. Drees, A. V. Fedotov,
W. Fischer, C. Folz, D. Gassner, X. Gu, R. Gupta, Y. Hao, C. Hetzel, D. Holmes, H. Huang,
J. Kewisch, Y. Li, C. Liu, H. Lovelace III, Y. Luo, G. Mahler, D. Marx, F. Meot, M. Minty,
C. Montag, S. Nayak, R. B. Palmer, B. Parker, S. Peggs, B. Podobedov, V. Ptitsyn,
V. H. Ranjbar, G. Robert-Demolaize, M. Sangroula, S. Seletskiy, K. S. Smith, S. Tepikian,
R. Than, P. Thieberger, N. Tsoupas, J. Tuozzolo, S. Verdu-Andres, E. Wang, D. Weiss,
F. J. Willeke, H. Witte, Q. Wu, W. Xu, A. Zaltsman
Brookhaven National Laboratory, Upton, NY 11973, USA
S. Benson, B.R.P. Gamage, J. Grames, T. Michalski, E. Nissen, J. Preble, R. Rimmer,
T. Satogata, A. Seryi, M. Wiseman, W. Wittmer
TJNAF, Newport News, VA 23606, USA
V. Morozov, F. Lin, Oak Ridge National Laboratory, Oak Ridge, TN 37831, USA
E. Gianfelice-Wendt, Fermi National Accelerator Laboratory, Batavia, IL 60510, USA
Y. Cai, Y. Nosochkov, G. Stupakov, M. Sullivan, SLAC, Menlo Park, CA 94025, USA
J. Qiang, Lawrence Berkeley National Laboratory, Berkeley, CA 94720, USA
G. Hoffstaetter, D. Sagan, M. Signorelli, J. Unger, Cornell University, Ithaca, NY 14850, USA

Abstract

The Electron Ion Collider (EIC) under construction at Brookhaven National Laboratory aims to produce luminosities of up to 10^{34} cm^{-2}s^{-1} . The machine will operate over a broad range of collision energies with highly polarized beams. The coexistence of highly radiative electrons and nonradiative ions produces a host of unique effects. In order to maximize the luminosity, the beam-beam collision parameters are pushed to limits achieved only in collisions with equal species. Moreover, collisions occur with a 25 mrad crossing angle; the resulting luminosity reduction is compensated to lowest order by crabbing both beams by means of transverse RF oscillators. Keeping the beams stable under these conditions is challenging. The average polarization of electron and light ion beams must be 70%. Beams therefore must be injected fully polarized and polarization must be well preserved during beam acceleration and collision. Electron beam currents are up to 2.5 A, which is associated with a number of collective effects that need to be controlled. Hadron beam currents of 1 A are effected by the electron cloud effect, which will be suppressed by low secondary electron-emission yield (SEY) vacuum chamber coating. Strong hadron cooling will reduce and stabilize the hadron beam emittance and will boost the luminosity by a factor of three. These are some of the accelerator science challenges and the corresponding cures and resolutions that are described in this report.

INTRODUCTION

EIC, an ultimate electron microscope to be built at Brookhaven National Laboratory, provides the capability to look inside the nucleon. The EIC enables the study of the contribution of quarks and gluons to nucleon spin and mass. To answer this question, achieving high luminosity from polarized beams with variable center-of-mass energy is essential [1].

The center-of-mass energy in electron-proton collisions ranges from 29 to 141 GeV, accomplished by colliding $5 - 18$ GeV electrons with $41 - 275$ GeV ions. The peak luminosity is 10^{34} cm^{-2}s^{-1}, which will be achieved by colliding 10 GeV electrons with 275 GeV protons. Two IRs are considered in EIC. The first one is designed at IR6, and the second one is reserved at IR8 for future upgrade.

Figure 1 presents the schematic diagram of the EIC layout. Ion beams from protons to uranium will be accelerated to desired energy and stored in the Hadron Storage Ring (HSR), which will use existing RHIC complex. Strong Hadron Cooling will be used to maintain the required emittance of the flat hadron beam. An Energy Recovery LINAC (ERL) is being designed to provide electron beams for cooling. The Electron Storage Ring (ESR), which will be installed in the existing RHIC accelerator tunnel, will operate at three fixed energies. The polarized electrons will be injected from the Rapid Cycling Synchrotron (RCS) [2].

LUMINOSITY

In EIC, electron and hadron beams will cross with a horizontal angle of 25 mrad to avoid parasitic collisions. Crab cavities tilt the ion and electron bunches in the $z - x$ plane by half the crossing angle to compensate for the geometric luminosity loss, as shown in Fig. 2. Table 1 lists the key

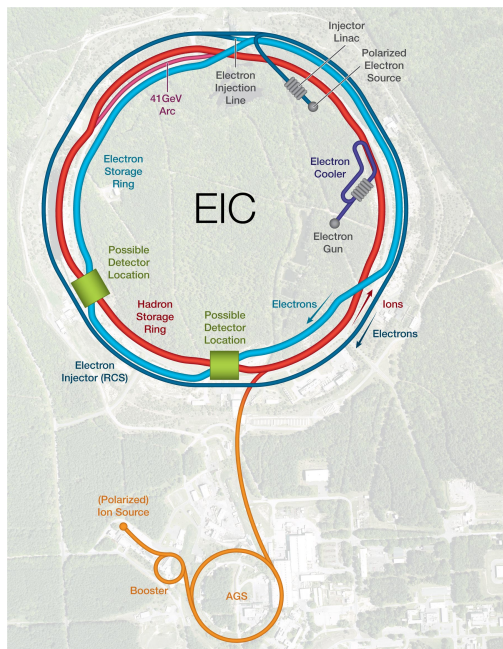**MC1: Circular and Linear Colliders**

A19: Electron - Hadron Colliders

Figure 1: Schematic layout of EIC accelerator systems.

Table 1: EIC Key Design Parameters for Highest Luminosity

Parameter	Unit	Proton	Electron
Circumference	m	3833.89	3833.98
Particle energy	GeV	275	10
Bunch intensity	10^{11}	0.668	1.72
# of Bunches	-	1160	
Crossing angle	mrad	25	
β^* at IP	cm	80/7.2	45/5.6
σ_x^*/σ_y^* at IP	μm	95/8.5	
Bunch length σ_z	cm	6	2
Energy spread σ_δ	10^{-4}	6.6	5.5
Transverse tunes	-	0.228/0.210	0.08/0.06
Longitudinal tune	-	0.01	0.069
Beam-beam parameter	-	0.012/0.012	0.07/0.10
Luminosity	$cm^{-2}s^{-1}$	10^{34}	

parameters to achieve the highest luminosity. The corresponding beam-beam parameters are 0.1 for electrons, and 0.012 for protons. Similar beam-beam parameters have been successfully demonstrated in routine operations at lepton or hadron colliders, such as KEKB, RHIC and LHC [3–5]. Their successful combination in EIC has been demonstrated by weak-strong and strong-strong simulations [6].
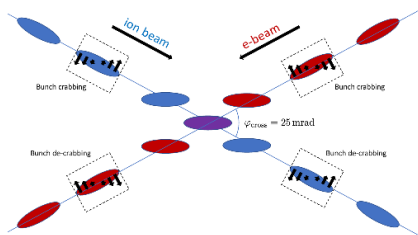

Figure 2: EIC local crabbing compensation scheme.

Synchro-betatron resonances have to be avoided in the hadron beam. Particles in the head and tail of the proton bunch have different horizontal offsets due to the sinusoidal waveform from the crab cavity voltage,

$$\Delta x = -\theta_c \left[\frac{\sin(k_c z)}{k_c} - z \right] \quad (1)$$

where θ_c is the half crossing angle, and k_c is the crab cavity wave number.

There are two kinds of synchro-betatron resonances excited by nonlinear horizontal offset: $m\nu_x + p\nu_z = 1$ and $2(\nu_x - \nu_y) + p\nu_z = 0$ [7], where $\nu_{x,y,z}$ are tunes. The first causes significant horizontal emittance growth, while the second contributes vertical emittance growth. Theoretical studies and simulations suggest that the emittance growth is

mitigated if the working point moves to $(0.228, 0.210)$. The leading resonance line for this working point is $4\nu_x + p\nu_z = 1$. The second family of synchro-betatron resonances is also weak as the working point is far from the main diagonal line. The second order harmonic crab cavity, which can be used to flatten the nonlinear offset, turns out to be useful in weak-strong simulations [8].

Beam-beam interactions can cause coherent instabilities. We carried out a systematic tune scan of the electron beam with the fixed tunes of the proton beam [9]. The electron horizontal tune must avoid the range from 0.1 to 0.14. The nominal electron working point $(0.08, 0.06)$ avoids vertical size blow-up and coherent beam-beam instability.

The second IR is reserved for EIC future upgrade. However, with the same beam-beam parameters, the sum luminosity will be reduced to half when the bunches collide twice per turn. A possible method is to change the electron bunch filling patterns [10]. By shifting the half electron bunches with 3 RF buckets, each bunch will collide at either IR6 or IR8, and two IRs will share the total luminosity. Figure 3 shows the collision pattern.
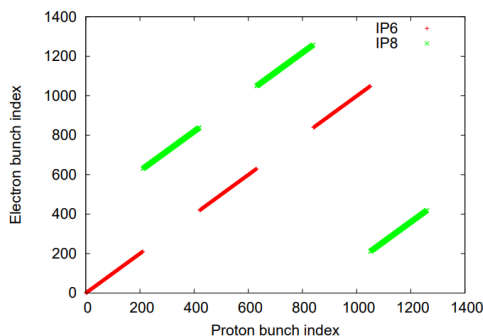

Figure 3: Collision pattern with two IRs in EIC.

To remove some of physical interferences between rings, transfer lines, and cooler ERL in IR2, ESR is proposed to

MC1: Circular and Linear Colliders

A19: Electron - Hadron Colliders

be tilted by ~ 200μrad to avoid vertical bends. Figure 4 illustrates the concept. The rotating axis goes through both interaction points: IP6 and IP8. Additional vertical crabbing is needed to compensate for the luminosity loss and avoid proton emittance growth [11].
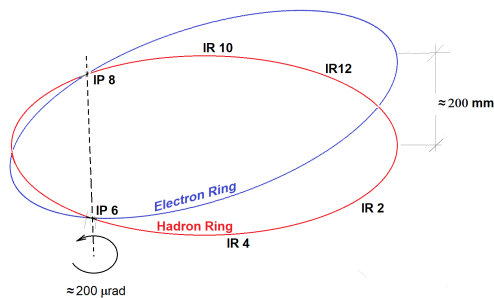

Figure 4: Schematic diagram of the ESR tilt.

POLARIZATION

The EIC physics program requires highly polarized hadron and electron beams with alternating spin orientation for the electron bunches. The present hadron injector, the Alternating Gradient Synchrotron (AGS), will be reused for EIC. RHIC has provided polarized proton beams over a wide energy range during the past decade [12]. Four additional Siberian snakes for a total of six snakes will be installed in HSR. With a proper arrangement of snakes in HSR and an additional reduction of emittance growth in AGS, the polarization is expected to reach 70% at 275 GeV beam energy. This upgrade also allows the operation of polarized deuteron and ^{3}He beams. Spin rotators based on helical dipole magnets will be used to transform the vertical beam polarization in the arcs into longitudinal polarization at IP [13].

Polarized electrons are produced in the source with 85% longitudinal polarization [14]. The RCS, which injects at full energy into the ESR, is designed to be free of intrinsic spin resonances in the entire energy range from 400 MeV to 18 GeV. This is accomplished by enforcing a 96-fold lattice periodicity [15].

The electron bunches are injected into the ESR with high transverse polarization of 85% in the desired spin direction. The Sokolov-Ternov self-polarization process leads to a build-up of electron polarization in the direction opposite to the vertical guiding field. Stochastic photon emission leads to a randomization of the particle spin directions. As a result, the polarization varies with time as

$$P(t) = P_\infty \left(1 - e^{-t/\tau}\right) + P_0 e^{-t/\tau} \qquad (2)$$

where P_∞, $1/\tau$, and P_0 are the asymptotic polarization, the polarization rate, and the initial polarization, respectively. At 18 GeV with the refill time of 2.5 minutes, 16% asymptotic polarization corresponds to 70% average polarization. Spin simulation with magnet errors shows that the average polarization of at least 70% is achievable with one IR [16].

Studies with two IRs are underway. The transient effects of electron beam replacement on proton beam emittance is small (< 1%) with realistic injection errors [17].

LINEAR BEAM OPTICS

The main challenges of IR design are to fulfill multiple purposes with very tight space, as shown in Fig. 5. The β functions are strongly focused at IP. The crab cavities require high β_x, specific horizontal phase advance, and enough installation space. The IR also has to accommodate spin rotators and the detector [18, 19].
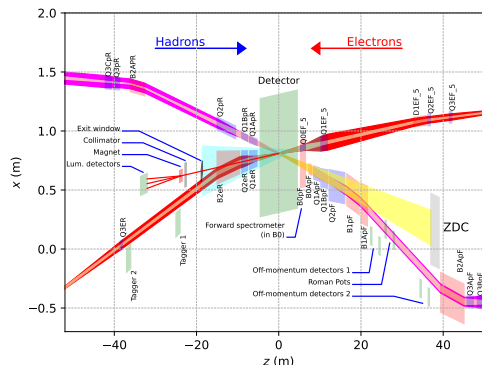

Figure 5: Layout of the EIC IR6.

Crab cavities impart $z-$dependent transverse kicks. We can define the crab dispersion as [20]

$$\zeta = \left(\frac{\partial x}{\partial z}, \frac{\partial x'}{\partial z}, \frac{\partial y}{\partial z}, \frac{\partial y'}{\partial z}\right) \qquad (3)$$

The crab dispersion closure is a challenge. Ideally, two thin crab cavities separated by $n\pi$ phase advance form a closed crab dispersion bump. Due to the tight space constraint, the horizontal phase cannot match exactly to $\pi/2$ in both ESR and HSR. The downstream crab cavity has to be moved to ~ $3\pi/2$ to close the bump in ESR. In HSR, there is no space to move away the crab cavities. The crab dispersion bump is not closed. As a result, the crab cavity voltages are adjusted to match the condition $\zeta^* = (12.5 \text{ mrad}, 0, 0, 0)$.

The vertical crabbing is another issue. Many sources lead to non-zero vertical crab dispersion, such as the tilted ESR and the detector solenoid. Vertical crab dispersion will couple the longitudinal and vertical dynamics, resulting in a significant luminosity loss. Skew quadrupoles are feasible and efficient to control vertical crabbing. In ESR, the required skew component strength is 1.2 T/m [21]. In HSR, it may combine with the global decoupling system.

The crab dispersion is distorted by RF phase and amplitude noise. RF noise causes the transverse emittance growth which is proportional to the crossing angle squared [22]. Compared with High-Luminosity LHC, EIC sensitivity to RF noise is 4000 times higher, and the emittance growth tolerance is 3 orders of magnitude higher. The RF noise threshold for the HSR will be hard to achieve. A dedicated feedback system is needed [23].

Designing spin rotators for a broad range of energies is also a challenge. ESR spin rotator design is based on a combination of solenoids and horizontal bending magnets. Figure 6 shows the configuration of ESR spin rotator. In general, the spin precesses around vertical axis in dipoles, and longitudinal axis in solenoids. This structure is capable of rotating the spin from vertical axis to longitudinal axis in a wide energy range between 6 GeV and 18 GeV [24]. Spin matching of spin rotator optics minimizes beam depolarization, especially at 18 GeV [25].

Figure 6: ESR spin rotator configuration.

DYNAMIC APERTURE

HSR reuses arcs of both Yellow and Blue RHIC rings. The dynamic aperture of the hadron ring has been determined by particle tracking and benchmarked with similar calculations for RHIC data. The simulations demonstrate that the hadron beam has sufficient dynamic aperture after the linear chromaticity is corrected by two families of sextupoles. More sextupole families are available for further DA optimization [26].

However, IR magnetic field errors play an important role in hadron ring dynamic aperture reduction. Artificial random magnetic field errors are assigned to all IR dipoles and quadrupoles to evaluate their impacts on dynamic aperture. The tolerances are then determined from long term tracking with the beam-beam interaction.

The magnetic field error is defined as

$$\Delta B_y + \mathrm{i}\Delta B_x = B(R)\left[10^{-4}\sum_{n=0}^{N_{\max}}(b_n + \mathrm{i}a_n)\frac{(x+\mathrm{i}y)^n}{R^n}\right] \quad (4)$$

where R is the reference radius. Figure 7 shows the DA tracked by 10^6 turns with a momentum spread of $3\sigma_\delta$. Based on RHIC operational experience, simulated DA with
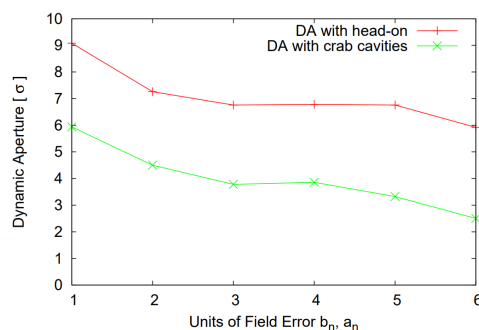

Figure 7: Dynamic aperture in HSR with IR magnetic field errors.

beam-beam should be better than 5σ to guarantee a decent proton beam lifetime. A 3σ drop in DA is observed from head-on to crabbed collision. With crab cavities, particles with $z \neq 0$ will see additional horizontal offset in IR magnets and sample larger IR field errors, which causes DA reduction. To minimize this effect, the IR field errors has to be controlled within 10^{-4} with $R = 60$ mm at dipoles and $R = 45$ mm for quadrupoles. [26].

In ESR, the optimization goal for dynamic aperture and momentum acceptance is chosen as 10σ in 3 planes. The DA of 18 GeV lattice with a 2nd IR is the most challenging one. The phase advance of the arc FODO cell is set to 60° at lower energies and 90° at 18 GeV. The stronger focusing enhances the chromaticity. The second IR results in a significantly large off-momentum β-beating. Although this can be mitigated by setting the phase advance between IPs to an odd multiple of 90°, the compensation is far from sufficient due to the asymmetry of the IRs. In particular, the RMS energy spread at 18 GeV is substantial, reaching 0.1%. It leads to the required momentum acceptance as large as $1\% \sim 10\sigma$. Furthermore, the fractional tunes, which are selected by beam-beam study and spin dynamics, cannot be used as free parameters in the optimization. Their closeness to integers makes chromatic compensation harder.

There is no space in IR for local chromatic compensation. The β-beating and chromaticity from the final focusing doublet are corrected in the neighbouring arc section. Phase trombones are needed to align the phase to the arc sextupoles. Harmonic sextupoles in IR2 are used to correct the third-order resonances. The second-order dispersion is corrected with two independent sextupoles [27].

Figure 8 shows the final dynamic aperture with all corrections. The design criteria of $\sim 10\sigma$ in all three planes is achieved for the 90° lattice at 18 GeV with two IRs.
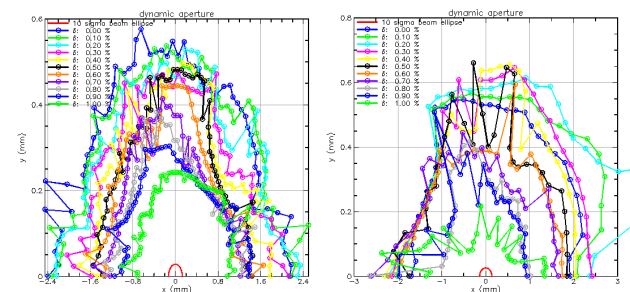

Figure 8: Dynamic aperture for ESR 18 GeV, left: bare lattice, right: with beam-beam interaction, crab cavity, detector solenoid, and crab dispersion control by skew quadrupoles. 10σ aperture is achieved in 3 planes.

COLLECTIVE EFFECTS

To achieve the luminosity of 10^{34} cm^{-2}s^{-1}, both desired beam currents – 1 A for protons, 2.5 A for electrons – are limited by collective effects. The calculation and optimization of various vacuum components are ongoing. The impedance budget is in progress [28].

In ESR, the single bunch instability threshold is above the requirement for stable operation. Beam-induced heating is a problem. Many components require water cooling. The beam-beam interaction provides a large tune spread to Landau damp transverse coupled-bunch [29] and ion instability [30]. The proton beam emittance growth is sensitive to the electron bunch arrival time jitter in the crab cavities. Therefore, a longitudinal damper is needed to limit coherent longitudinal beam oscillation in the presence of longitudinal coupled bunch instability [31].

With the current RHIC beam pipe, HSR is vulnerable to electron cloud instability and high resistive losses from beam-induced currents. The vacuum chamber of the HSR superconducting magnets and their cold interconnects will be updated with a beam screen to present sufficiently low impedance and low SEY [32].

Crab cavities produce a time varying horizontal kick that can lead to transverse coupled bunch instabilities. Figure 9 shows the growth rate of the transverse coupled bunch mode for a crab system with an external $Q = 3 \times 10^6$. An effective way is to add sufficient RF feedback to the crabbing RF system. Feedback with $Q_{\text{eff}} = 600$ appears adequate for the ESR crab cavities. In HSR, the adequate feedback is $Q_{\text{eff}} = 300$ for 197 MHz, and $Q_{\text{eff}} = 600$ for 394 MHz [33].
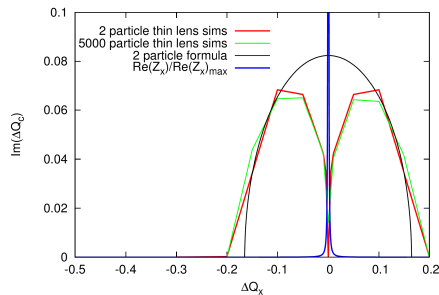

Figure 9: Growth rate versus horizontal fractional tune for the transverse coupled bunch mode of a crab system with an external $Q = 3 \times 10^6$, for 275 GeV protons with 3 different physical models. The blue line is the ratio of the transverse resistance to the peak value of the transverse resistance.

The number of macroparticles can influence the results of a simulation. In EIC, with no radiative damping, the dependence of the growth rates on the number of macroparticles has to be included in realistic studies. Figure 10 simulates the momentum spread versus the beam intensity in the presence of the longitudinal wake field for 5 GeV electrons. The actual momentum spread can be obtained by extrapolating the number of macroparticles to real particle numbers [34].

STRONG HADRON COOLING

To maintain a luminosity of 10^{34} cm^{-2}s^{-1}, it is necessary to cool the hadron beams to balance emittance growth rates due to Intrabeam Scattering (IBS) thereby allowing to keep the same hadron beam for long collision runs. With the parameters in Table 1, IBS longitudinal and transverse
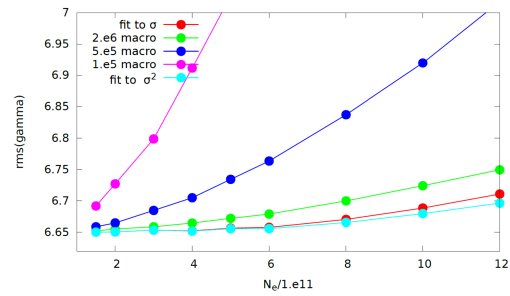

Figure 10: Simulation results for the RMS momentum spread versus beam intensity with different numbers of macro-particles.

growth times are $2 - 3$ hours. The cooling time must be equal to or less than the diffusion growth time from all sources. Strong Hadron Cooling (SHC) will boost the luminosity in the range of EIC by a factor of $3 - 10$, as shown in Fig. 11.
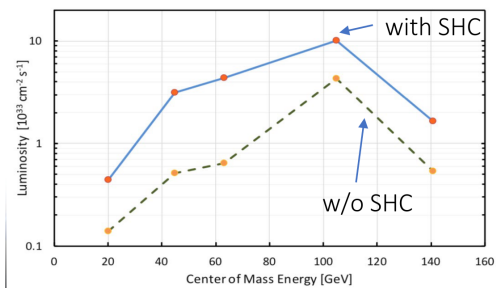

Figure 11: EIC electron-proton peak luminosity versus center-of-mass energy.

SHC is realized in the form of micro-bunched electron cooling. This scheme is essentially a high-bandwidth stochastic cooling system, with an electron beam acting as the pickup and kicker, and a micro-bunch instability used to amplify the imprint the protons leave on the electron beam in the pickup section. Accelerator design of the SHC is underway [35, 36].

ACKNOWLEDGMENT

REFERENCES

[1] A. Accardi *et al.*, "Electron-Ion Collider: The next QCD frontier", *Eur. Phys. J. A*, vol. 52 p. 268, 2016. doi:10.1140/epja/i2016-16268-9

[2] F. Willeke and J. Beebe-Wang, "Electron Ion Collider Conceptual Design Report 2021", Brookhaven National Lab., Upton, NY, USA, Tech. Rep. BNL-221006-2021-FORE, Feb. 2021. doi:10.2172/1765663

[3] K. Akai *et al.*, "SuperKEKB collider", *Nucl. Instrum. Methods Phys. Res. Sect. A*, vol. 907, pp. 188-199, 2018. 10.1016/j.nima.2018.08.017

MC1: Circular and Linear Colliders

A19: Electron - Hadron Colliders

[4] X. Gu *et al.*, "Electron lenses for head-on beam-beam compensation in RHIC", *Phys. Rev. Accel. Beams*, vol. 20, no. 2, p. 023501, 2017. `doi:10.1103/PhysRevAccelBeams.20.023501`

[5] R. Alemany *et al.*, "Head-on beam-beam tune shifts with high brightness beams in the LHC", CERN, Geneva, Switzerland, Rep. CERN-ATS-Note-2011-029 MD, May 2011.

[6] Y. Luo *et al.*, "Beam-beam related design parameter optimization for the electron-ion collider", in *Proc. 12th Int. Particle Accelerator Conf. (IPAC'21)*, Campinas, Brazil, May 2021, pp. 3808–3811. `doi:10.18429/JACoW-IPAC2021-THPAB028`

[7] D. Xu, Y. Hao, Y. Luo, and J. Qiang, "Synchrobetatron resonance of crab crossing scheme with large crossing angle and finite bunch length", *Phys. Rev. Accel. Beams* vol. 24 no. 4 p. 041002, 2021. `doi:0.1103/PhysRevAccelBeams.24.041002`

[8] D. Xu, Y. Hao, Y. Luo, C. Montag, and J. Qiang, "Study of harmonic crab cavity in EIC beam-beam simulations", in *Proc. 12th Int. Particle Accelerator Conf. (IPAC'21)*, Campinas, Brazil, May 2021, pp. 2595–2597. `doi:10.18429/JACoW-IPAC2021-WEPAB009`

[9] J. Qiang, Y. Luo, C. Montag, F. J. Willeke, D. Xu, and Y. Hao, "Strong-strong simulations of coherent beam-beam effects in the EIC", in *Proc. 13th Int. Particle Accelerator Conf. (IPAC'22)*, Bangkok, Thailand, Jun. 2022, paper WEPOPT041, this conference.

[10] Y. Luo, M. Blaskiewicz, A. He, C. Montag, and V. Ptitsyn, "Beam-beam issues with two interaction points in eRHIC", in *Proc. 9th Int. Particle Accelerator Conf. (IPAC'18)*, Vancouver, Canada, Apr.-May 2018, pp. 102–104. `doi:10.18429/JACoW-IPAC2018-MOPMF011`

[11] D. Xu and Y. Luo, "Beam-Beam Interaction for Tilted Storage Ring", in *Proc. 13th Int. Particle Accelerator Conf. (IPAC'22)*, Bangkok, Thailand, Jun. 2022, paper WEPOPT049, this conference.

[12] W. B. Schmidke *et al.*, "RHIC polarization for runs 9-17", Brookhaven National Lab., Upton, NY, USA, Tech. Rep. BNL-209057-2018-TECH, 2018.

[13] V. Ptitsyn and J. S. Berg, "EIC hadron spin rotators", in *Proc. 13th Int. Particle Accelerator Conf. (IPAC'22)*, Bangkok, Thailand, Jun. 2022, paper WEPOST020, this conference.

[14] E. Wang *et al.*, "The design of a high charge polarized preinjector for the Electron-Ion Collider", in *Proc. 12th Int. Particle Accelerator Conf. (IPAC'21)*, Campinas, Brazil, May 2021, pp. 1428–1430. `doi:10.18429/JACoW-IPAC2021-TUPAB037`

[15] V. H. Ranjbar, H. Lovelace III, F. Meot, and F. Lin, "EIC's rapid cycling synchrotron spin tracking update", in *Proc. 13th Int. Particle Accelerator Conf. (IPAC'22)*, Bangkok, Thailand, Jun. 2022, paper THPOST004, this conference.

[16] E. Gianfelice-Wendt, prive communication.

[17] J. Qiang *et al.*, "Transient beam-beam effect during electron bunch replacement in the EIC", in *Proc. 12th Int. Particle Accelerator Conf. (IPAC'21)*, Campinas, Brazil, May 2021, pp. 3228–3231. `doi:10.18429/JACoW-IPAC2021-WEPAB252`

[18] H. Witte *et al.*, "The interaction region of the Electron-Ion Collider EIC", in *Proc. 12th Int. Particle Accelerator Conf. (IPAC'21)*, Campinas, Brazil, May 2021, pp. 2574–2577. `doi:10.18429/JACoW-IPAC2021-WEPAB002`

[19] B.R. Gamage *et al.*, "Design concept for a second interaction region for the Electron-Ion Collider", in *Proc. 13th Int. Particle Accelerator Conf. (IPAC'22)*, Bangkok, Thailand, Jun. 2022, paper MOPOTK046, this conference.

[20] Y.-P. Sun, R, Assmann, R. Tomás, and F. Zimmermann, "Crab dispersion and its impact on the CERN Large Hadron Collider collimation", *Phys. Rev. Accel. Beams*, vol. 13 no. 3, p. 031001, 2010. `doi:10.1103/PhysRevSTAB.13.031001`

[21] D. Xu *et al.*, "Detector solenoid compensation in the EIC electron storage ring", in *Proc. 13th Int. Particle Accelerator Conf. (IPAC'22)*, Bangkok, Thailand, Jun. 2022, paper MOPOPT050, this conference.

[22] P. Baudrenghien and T. Mastoridis, "Transverse emittance growth due to rf noise in the high-luminosity LHC crab cavities", *Phys. Rev. Spec. Top. Accel. Beams* vol. 18 no. 10, p. 101001, 2015. `10.1103/PhysRevSTAB.18.101001`

[23] K. Smith, "EIC Transverse emittance growth due to crab cavity RF noise: estimates and mitigation", Brookhaven National Lab., Upton, NY, USA, Tech. Rep. BNL-222748-2022-TECH, 2022.

[24] D. Marx *et al.*, "Designing the EIC electron storage ring lattice for a wide energy range", in *Proc. 13th Int. Particle Accelerator Conf. (IPAC'22)*, Bangkok, Thailand, Jun. 2022, paper MOPOPT042, this conference.

[25] D. Marx *et al.*, "Task Force Report: ESR Linear Lattice Design", Brookhaven National Lab., Upton, NY, USA, Tech. Rep. BNL-222485-2021-TECH, EIC-ADD-TN-025, 2021.

[26] Y. Luo *et al.*, "Dynamic aperture evaluation for the hadron storage ring in the Electron-Ion Collider", in *Proc. 12th Int. Particle Accelerator Conf. (IPAC'21)*, Campinas, Brazil, May 2021, pp. 3812–3814. `doi:10.18429/JACoW-IPAC2021-THPAB029`

[27] Y. Cai *et al.*, "Design of Chromatic Optics in Electron Storage Ring of the Electron-Ion Collider", submitted to *Phys. Rev. Accel. Beams*.

[28] A. Blednykh *et al.*, "An overview of the collective effects and impedance calculation for the EIC", in *Proc. 12th Int. Particle Accelerator Conf. (IPAC'21)*, Campinas, Brazil, May 2021, pp. 4266–4269. `doi:10.18429/JACoW-IPAC2021-THPAB238`

[29] R. Li and M. Blaskiewicz, "Impact of coherent beam-beam interaction on the Landau damping of the transverse coupled-bunch instability", in *Proc. 12th Int. Particle Accelerator Conf. (IPAC'21)*, Campinas, Brazil, May 2021, pp. 2062–2065. `doi:10.18429/JACoW-IPAC2021-TUPAB258`

[30] M. Blaskiewicz, "Beam-beam damping of the ion instability", in *Proc. North American Particle Accelerator Conf. (NAPAC'19)*, Lansing, MI, USA, Sep. 2019, pp. 391–394. `doi:10.18429/JACoW-NAPAC2019-TUPLM11`

[31] B. Podobedov, "Limiting coherent longitudinal beam oscillations in the EIC electron storage ring", B Brookhaven National Lab., Upton, NY, USA, Tech. Rep. BNL-215885-2020-TECH, 2020.

MC1: Circular and Linear Colliders

A19: Electron - Hadron Colliders

[32] S. Verdú-Andrés *et al.*, "A beam screen to prepare the RHIC vacuum chamber for EIC hadron beams: conceptual design and requirements", in *Proc. 12th Int. Particle Accelerator Conf. (IPAC'21)*, Campinas, Brazil, May 2021, pp. 2066–2069. doi:10.18429/JACoW-IPAC2021-TUPAB260

[33] M. Blaskiewicz, "Instabilities driven by the fundamental crabbing mode", Brookhaven National Lab., Upton, NY, USA, Tech. Rep. BNL-222221-2021-TECH, 2021.

[34] M. Blaskiewicz, private communication.

[35] S. Peggs *et al.*, "Optics for strong hadron cooling in EIC HSR-IR2", in *Proc. 13th Int. Particle Accelerator Conf. (IPAC'22)*, Bangkok, Thailand, Jun. 2022, paper WEPOPT035, this conference.

[36] W. F. Bergan, P. Baxevanis, M. Blaskiewicz, G. Stupakov, and E. Wang, "Design of an MBEC cooler for the EIC", in *Proc. 12th Int. Particle Accelerator Conf. (IPAC'21)*, Campinas, Brazil, May 2021, pp. 1819–1822. doi:10.18429/JACoW-IPAC2021-TUPAB179